Adv Polym Sci (2013) 261: 295–320
DOI: 10.1007/12_2013_255

Published online: 27 October 2013

Probing Macromolecular and Supramolecular Structure, Dynamics, and Function by Magnetic Resonance

Hans Wolfgang Spiess

Abstract The use of magnetic resonance spectroscopy, both electron paramagnetic resonance (EPR) and nuclear magnetic resonance (NMR) for elucidating the structure, dynamics, and function of macromolecular and supramolecular systems is described. The role of chain conformation in governing supramolecular organization is emphasized. Examples include polymers with conformational memory, polypeptides, dendronized polymers, as well as functional macromolecular and supramolecular systems for organic-based electronics. Acknowledging Hermann Staudinger's vision similarities between synthetic polymers and biopolymers, e.g., partially disordered proteins, are addressed. Moreover, the need to apply a multitude of techniques in studying the structure and dynamics of such complex systems is emphasized.

Keywords Biopolymers · Dynamics · Electron paramagnetic spectroscopy · NMR spectroscopy · Polymers · Structure

Contents

1 Introduction 296
2 Solid State NMR and Pulsed EPR Techniques for Analyzing Structure and Dynamics . 297
3 Structure and Dynamics of Macromolecular Systems Governed by Their Local Conformations 298
3.1 Conformational Memory in Synthetic Polymers 298
3.2 Self-Assembly and Dynamics of Polypeptides 302
3.3 Protein Dynamics and Flexibility: Order and Disorder in Proteins 304
3.4 Dendronized Polymers 306

H.W. Spiess
Max-Planck-Institute for Polymer Research, P. O. Box 3148, 55021 Mainz, Germany
e-mail: spiess@mpip-mainz.mpg.de

4 Functional Materials 309
4.1 Elastin-Like Polypeptides and Drug Delivery 309
4.2 Columnar Stacks 311
4.3 Pi-Conjugated Macromolecules for Organic Electronics 313
5 Conclusion 316
References 317

1 Introduction

To state that precise knowledge of the structure and dynamics of macromolecules of well-defined architectures is of utmost importance when tailoring them for specific functions nowadays sounds like *ululas Athenas portare*. In his Nobel lecture in 1953 on macromolecular chemistry [1] Hermann Staudinger emphasized the importance of determining the *structure* of macromolecules, but did not mention their *dynamics*. He listed several experimental techniques for determining the structure and the molecular weight of macromolecules that were in use at that time, when the macromolecular nature of both synthetic and biomacromolecules was under debate, but magnetic resonance was not among them. This is easily explained by the fact that magnetic resonance (MR) techniques based on electron spins (i.e., electron paramagnetic resonance, EPR, spectroscopy) and on nuclear spins (i.e., nuclear magnetic resonance, NMR, spectroscopy) were in their infancies, being discovered in 1944 by E. K. Zavoisky [2], and in 1945 by F. Bloch and E.M. Purcell, respectively [3, 4]. Naturally, their potential in macromolecular science was not yet known. As early as the 1960s, however, G. Natta and coworkers took advantage of the new NMR technique to elucidate the stereoregularity of poly(propylene) [5], providing a new way of structural characterization of macromolecular chains [6]. Polymer dynamics is closely linked to the mechanical properties of polymer materials [7]. As molecular dynamics leads to narrowing of NMR lines, the analysis of ^{1}H NMR line shapes of bulk polymers offered a means for a better understanding of these delicate relationships [8]. Indeed, as early as 1959, W. P. Slichter published a seminal paper [9], again in Staudinger's journal, entitled "Nuclear resonance studies of motion in polymers," describing these developments. Much later, ^{2}H NMR on selectively deuterated polymers provided unique possibilities for elucidating both the time scale and geometry of molecular dynamics in polymers [10].

Today, NMR spectroscopy has advanced to become an indispensable tool in polymer research. The introduction of Fourier transform NMR and its extension to two and higher dimensions [11] made it possible to include low-sensitivity, yet highly informative, spectroscopy of rare nuclei such as ^{13}C or ^{15}N. These techniques are now mainly applied to study biomacromolecules [12] in solution, but increasingly also in the solid state [13]. In the latter case, multidimensional NMR techniques were actually developed first for synthetic polymers [14]. Later, advances in solid state

NMR under fast magic angle spinning (MAS) offered an attractive way to elucidate the packing and local dynamics of the building blocks in supramolecular assemblies [15]; for a review of the early examples see [16].

In the early days of magnetic resonance, NMR and EPR spectroscopy were developed in parallel and often by the same people [17, 18]. Later on, the two techniques largely separated, but recent developments in microwave technology have allowed spectroscopists to use pulse methods in EPR as well [19] and it is rewarding to see the two "sister spectroscopies" merge again. In fact, the current revival of EPR (ESR) spectroscopy in macromolecular science [20–22] is largely due to the development of pulsed methods by groups active in both solid state NMR and EPR [23, 24]. Using these techniques, together with site-directed spin labeling [25], the structure of biomacromolecules and supramolecular assemblies can now be probed on the nanometer scale, which nicely augments the subnanometer information provided by NMR. A singular advantage of MR methods is the fact that structure determination does not require single crystals, as needed for X-ray diffraction or neutron scattering [26]. Therefore, MR can be applied to condensed matter in all forms: liquids, crystalline solids, disordered solids, liquid crystals, and even gases.

This chapter collects a few recent studies on the structure and dynamics of macromolecular and supramolecular systems, largely based on the author's group in collaboration with other more synthesis-oriented colleagues. For additional reading we refer to a recent perspective article [27] and recent reviews [28–30]

2 Solid State NMR and Pulsed EPR Techniques for Analyzing Structure and Dynamics

Signals originating from hydrogen-bonded protons are well separated in ^{1}H MAS NMR spectra, typically resonating between 8 and 20 ppm [11, 16]. Therefore, the ^{1}H chemical shift provides semiquantitative information about the strength of the hydrogen bonds. In addition, the ^{1}H chemical shift is also a sensitive probe of so-called ring currents associated with aromatic moieties [16]. They are observed as a low field shift compared to the corresponding liquid state signal and may thereby serve as a direct hint for π–π interactions. Likewise, the low field shift can be simply related to the packing via so-called nucleus independent chemical shift (NICS) maps [31]. This augments the well-known sensitivity of ^{13}C NMR chemical shifts to local conformation [6], known as the "γ-gauche effect". Detailed packing information is obtained from distance measurements between specific proton sites at adjacent building blocks via high resolution double quantum (DQ) solid state NMR under MAS [16, 28]. This is particularly important for supramolecular assemblies involving aromatic groups and functional polymers for organic electronics [32, 33].

Solid state NMR, however, is probably even more powerful for probing the time scale and geometry of rotational motions [14]. For instance, disk-shaped aromatics often stack into columnar structures as part of discotic liquid crystals (DLC)

[34]. In the liquid crystalline phase, the disks rotate around the column axis. A particularly simple way of characterizing such restricted molecular dynamics is provided by the dynamic order parameter S, $0 \leq S \leq 1$. It is defined as the ratio between the motionally averaged and the static anisotropic NMR interaction, e.g., dipole–dipole coupling, anisotropic chemical shift, or quadrupole coupling [14]. For the rotation of disks in a perfectly packed column, $S = 0.5$ for ^{13}C–^{1}H dipole–dipole coupling or ^{2}H quadrupole coupling, centered around the C–H (C–D) bond direction. Imperfections of the packing in the liquid crystalline phase, where disks can be inclined to the column axis, lead to reduction of S below 0.5 and values as low as 0.15 have been found [35]. Thus, S provides both dynamic and structural information. In general, solid state NMR yields site selective information about the amplitude and time scales of molecular motions over broad ranges of length and time; for a recent review see [30].

The information about the structure and dynamics of polymers that EPR can provide is very similar [19, 21]. For synthetic polymers, biopolymers, and supramolecular assemblies, nitroxide spin probes and spin labels are particularly useful [36]. In solution, their EPR spectra are governed by the g-factor and the hyperfine splitting (denoted as a) to the ^{14}N nucleus of the NO group. In solution, the former determines the frequency of the center of the triplet arising from the hyperfine coupling. Both parameters are sensitive to the electronic environment. In the solid state, the anisotropy of the g-tensor leads to broad characteristic EPR line shapes, similar to those in solid state NMR. Likewise, the EPR spectra are averaged by rotational motions, yet on time scales in the nanosecond scale rather than the microsecond scale that is relevant in NMR [14, 19]. This motional averaging has been exploited extensively in macromolecular science, due to the pioneering work of J. Freed [37]. Moreover, similar to NMR, the dipole–dipole couplings between electron and nuclear spins can be exploited to determine intermolecular distances below 1 nm. The much stronger couplings between two electron spins can probe distances up to about 8–10 nm. Both types of measurements are achieved by pulsed electron–nuclear or electron–electron double resonance techniques [23, 24], respectively.

3 Structure and Dynamics of Macromolecular Systems Governed by Their Local Conformations

3.1 Conformational Memory in Synthetic Polymers

In flexible polymers, the chains tend to form random coils and the local conformations allow isotropic rotational motions of the residues by a combination of angular fluctuations and conformational transitions [14, 38]. Stiff macromolecules with flexible side groups, however, lack conformational freedom within the backbone,

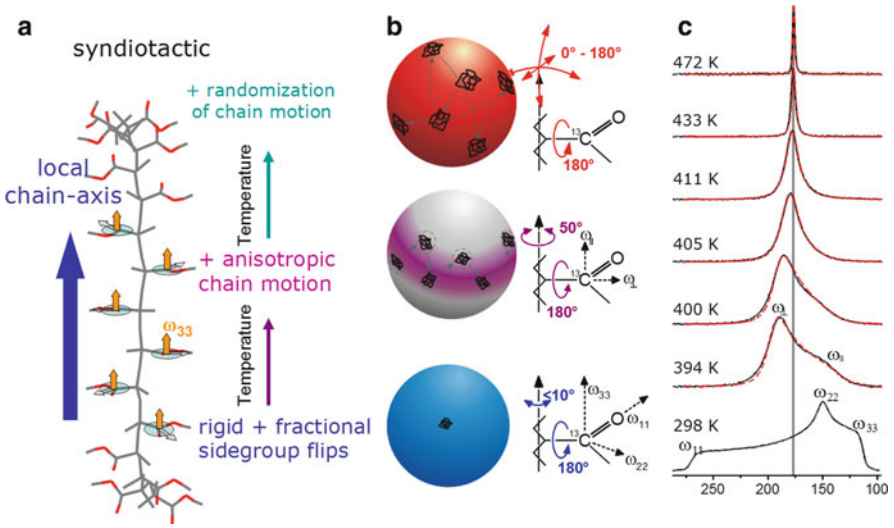

Fig. 1 (**a**) Extended chain conformation of syndiotactic poly(*n*-alkyl methacrylates). (**b**) Anisotropic chain motion during glass process. (**c**) ^{13}C NMR spectra indicating anisotropic motion above T_g, as described in the text

which leads to formation of layered structures even in the melt and highly anisotropic motion [39]. The question then arises whether in more conventional polymers extended conformations involving several repeat units can exhibit conformational memory manifesting itself in collective anisotropic motions. Randomization of conformation leading to locally isotropic reorientation could then occur as a separated process on a longer time scale. Structurally heterogeneous poly(*n*-alkylmethacrylates), which consist of a polar backbone and flexible nonpolar side groups $R_n = C_nH_{2n+1}$, are candidates for polymers with conformational memory, and indeed exhibit unusual relaxation behavior [40]. The backbone of these polymers contains extended syndiotactic sequences, which lead to extended chain conformations (see Fig. 1a).

Molecular dynamics of a macromolecular chain involves both conformational and rotational motions. Along these lines, the backbone dynamics of poly(*n*-alkyl methacrylates) has been elucidated by advanced solid state NMR, which enables conformational and rotational dynamics to be probed separately [41]. The former is encoded in the isotropic ^{13}C chemical shift. The latter is probed via the anisotropic ^{13}C chemical shift [14] of the carboxyl group with unique axis along the local chain direction. Randomization of conformations and isotropization of backbone orientation occur on the same time scale, yet they are both much slower than the slowest relaxation process of the polymer identified previously by other methods [40]. This effect is attributed to extended backbone conformations, which retain conformational memory over many steps of restricted locally axial chain motion (Fig. 1b, c). These findings were rationalized in terms of a locally structured polymer melt, in

which the polar and less flexible polymethacrylate backbones form disordered layers. This structure has been confirmed through temperature-dependent wide-angle X-ray scattering (WAXS) [42]. The anisotropic chain motion occurs within the layers; conformational randomization and rotational isotropization require extended chain units to translate from one structured unit to another. The variation in the molecular weight of PEMA showed that a minimum chain length of five to ten repeat units is required for this effect to occur [43]. In the vicinity of the glass transition temperature (T_g), the time scales of the two processes for PEMA differ by more than an order of magnitude, where the anisotropic motions follows a simple Arrhenius law and the isotropization process follows the Williams–Landel–Ferry (WLF) equation [7].

Recently, such peculiar chain dynamics were studied in nanoparticles onto which PEMA was grafted [44]. Through selective ^{13}C labeling, different parts of the PEMA brush were labeled: at the particle surface (brush A), in the middle (brush B), and at the chain end (brush C). In both brush A and brush B the isotropization is significantly slowed down, in particular at elevated temperatures (see Fig. 2a, b). The increased curvature of the data indicates a significant increase of T_g by about 20 K as well as significant changes in WLF parameters. Remarkably, the part of the chain directly bound to the surface, brush A, consisting of about 40 repeat units, displays virtually identical reduction in isotropization mobility as the part in the middle of the brush, brush B, where the labeled part is separated from the core by about 60 repeat units. This is remarkable because the nanostructures of PEMA mentioned above involve five to ten repeat units only.

This suggests that these structures, which are the reason for the clear separation of the time scales of the local chain motion and the isotropization in PEMA, are significantly affected by the presence of the nanoparticle. One can compare this effect with the significant reduction in the chain reptation in star polymers, where the star point does not move and chain motion can only occur via arm-retraction [45]. In fact, from ^2H NMR on selectively deuterated four-arm star poly(butadiene), Brereton el al. [46] found a similar behavior, namely almost uniform dynamics for the middle part of the arm, yet significantly shorter correlation times for the chain ends. Our work also motivated computer simulation of chain dynamics of grafted chains. It was found that the repeat units at the end relax faster than units further inside along the chain, as previously observed for planar brushes but at variance with theoretical expectations [47].

This example of studying polymer chain dynamics by advanced NMR techniques illustrates what kind of unique information this technique can provide. Many different types of information are accessible and its site selectivity is unmatched by other methods. In addition to the local dynamics, chain motion on mesoscopic length scales in polymer melts have been elucidated by various NMR techniques including DQ NMR in high and low magnetic fields [29, 48]. Last, but not least, the translational motion of poly(ethylene) chains from the crystalline to the noncrystalline regions and vice versa has been quantified in samples of different morphology, unraveling the decisive role of the interface [49].

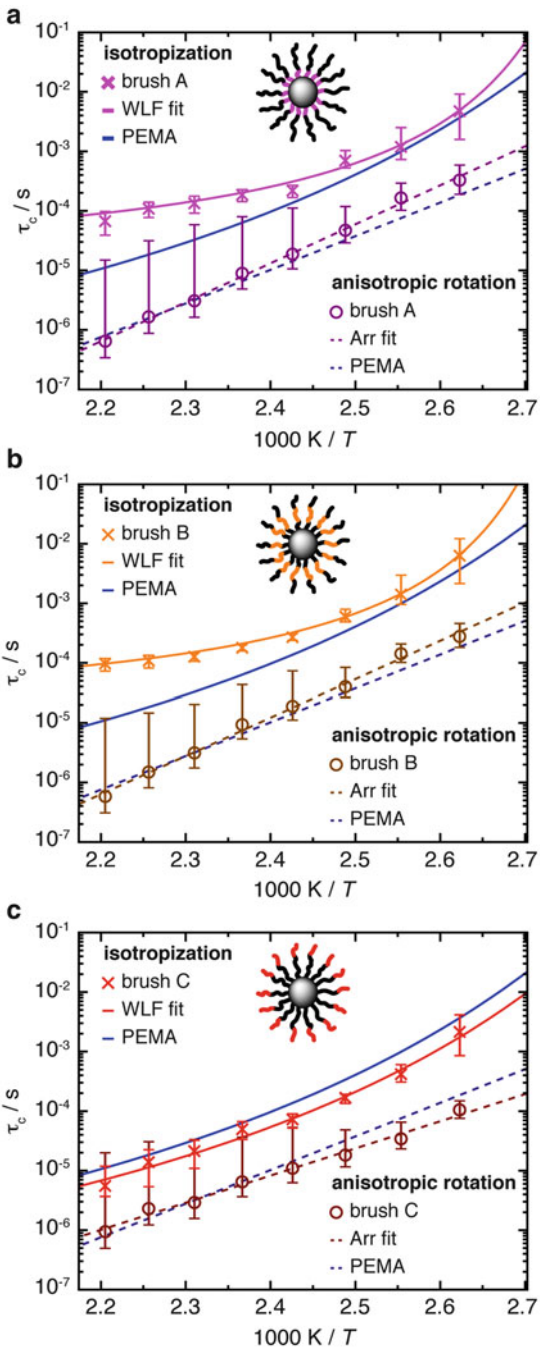

Fig. 2 Arrhenius plots of the two dynamic processes (isotropization and ansiotropic chain motion) for (**a**) brush A labeled at the particle surface, (**b**) brush B labeled in the middle of the brush shell, and (**c**) brush C labeled at the chain ends. For details see [44]

3.2 Self-Assembly and Dynamics of Polypeptides

It is remarkable that Hermann Staudinger had already considered synthetic and biomacromolecules in parallel and noted their similarities as well as their differences [1]. Following this, we note that local chain conformations also play a vital role in the organization of polypeptides, i.e., macromolecules composed of amino acids. Resembling biomacromolecules, they are considered for use in drug delivery and gene therapy and thus have been the subject of intensive studies [50, 51]. In addition, it is known that the superb performance of biological polypeptide-based materials such as hair or spiders' silk is due to a hierarchical superstructure over several length scales, where structure control is exerted at every level of hierarchy [52]. The two most common local conformations of polypeptides, known as secondary structures, are the α-helix, stabilized by intramolecular hydrogen bonds, and the β-sheet, stabilized by intermolecular hydrogen bonds. These secondary structures can be probed directly by solid state NMR [14] and their packing can be obtained from X-ray studies [53]. In addition, the α-helical structure posts a permanent dipole moment along its backbone and can, therefore, be classified as a type-A polymer in Stockmayer's classification [54]. This dipole moment can be measured precisely using dielectric spectroscopy (DS) and can be used as a probe of the persistence length of the secondary structure [55]. Over the years, we have studied various polypeptides by different NMR techniques, X-ray scattering, and dielectric spectroscopy [8] in order to better understand their hierarchical self-assembly (Fig. 3).

As shown in an extended review [56], the concerted application of these techniques has shed light into the origin of the glass transition, the persistence of the α-helical peptide secondary motif, and the effects of topology and packing on the type and persistence of secondary structures. Protein function and application often depend on these issues. Using poly(γ-benzyl-L-glutamate), PBLG, as an example, it was shown that helices are objects of rather low persistence in the bulk as well as in concentrated solutions in helicogenic solvents.

Copolypeptides, on the other hand, with their inherent nanometer length scale of phase separation, provide means of manipulating both the type and persistence of peptide secondary structures. As examples, we refer to the partial annihilation of α-helical structural defects due to chain stretching, to the induced chain folding of β-sheets in block copolypeptides with incommensurate dimensions, and to the destabilization of β-sheets in peptidic blocks having both secondary motifs [57, 58]. These effects should be taken into account when such peptides are going to be employed. in applications such as drug delivery.

Proline residues are of exceptional significance in protein conformation and protein folding because proline is the only amino acid where the nitrogen bears no amide hydrogen, preventing hydrogen bonding. Furthermore, the bulky pyrrolidine ring restricts the available conformations. Therefore, polypeptides with proline residues offer a unique possibility for unraveling the interplay between hydrogen bonding and geometric packing effects. In a recent multi-technique study of diblock copolymers of PBLG and poly(L-proline) (PLP) their hierarchical self-assembly was

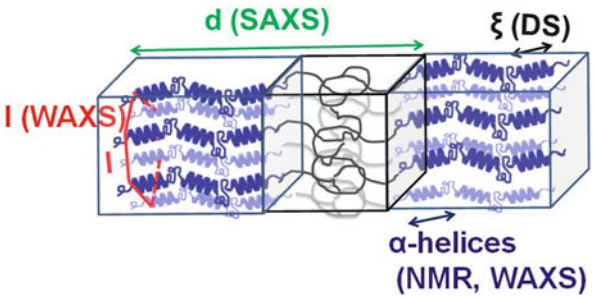

Fig. 3 Assembly of a lamellar-forming polypeptide-coil diblock copolymer, depicting the main techniques employed in our studies. Small-angle X-ray scattering (SAXS) is employed for the domain spacing, *d*. ^{13}C NMR and wide-angle X-ray scattering (WAXS) are employed to identify the type of peptide secondary structure (α-helical in the schematic). WAXS is further employed to specify the lateral self-assembly of α-helices within the polypeptide domain (a hexagonal lattice is indicated in the schematic). Dielectric spectroscopy (DS) and site-specific NMR techniques are employed for the dynamics. Furthermore, the most intense DS process provides the persistence length, l_p, of α-helical segments [56]

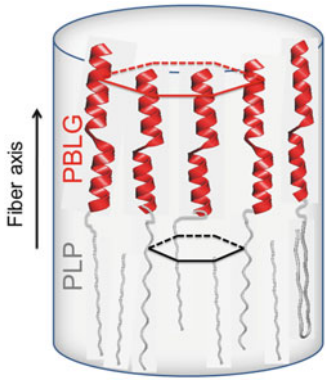

Fig. 4 Copolymer self-assembly, showing PBLG and PLP α-helices (NMR, WAXS) that are packed (WAXS) with significantly differently sized hexagons. The respective unit cells are indicated. The *arrow* indicates the fiber axis. Adopted from [59]

investigated. Both blocks possess helices stabilized either by hydrogen bonds (PBLG) or by steric hindrance (PLP) and are packed in two hexagonal cells of different dimensions. An intriguing *trans–cis* conformational change of PLP upon confinement was observed that mimics the isomerization of isolated proline residues in proteins. These *cis*-PLP conformations reside primarily at the PLP/PBLG interface, alleviate the packing frustration (see Fig. 4), and permit PBLG and PLP helices to pack with the bulk [59].

3.3 *Protein Dynamics and Flexibility: Order and Disorder in Proteins*

Hermann Staudinger concluded his Nobel lecture [1] by saying "macromolecular chemistry makes use of a number of qualitative correlations: those of shape and of the associated configurational scope, up to the level of the "atomos" of living substance, on which the game of Life ensues. In the light of this new knowledge of macromolecular chemistry, the wonder of Life in its chemical aspect is revealed in the astounding abundance and masterly macromolecular architecture of living matter." Thus, he clearly looked at synthetic macromolecules and biopolymers in parallel and looked for synergies in their understanding [60]. Moreover, self-organization and dynamics are common aspects in synthetic and biological systems alike [61, 62].

As far as proteins are concerned, the wealth of structural data available today [63] are from X-ray studies of protein single crystals. However, as stated in an extended review [64], the occurrence of unstructured regions of significant size (>50 residues) is surprisingly common in functional proteins. These disordered regions are characterized by great structural flexibility and plasticity. Obvious similarities between proteins and synthetic polymers are that both classes span a wide range of organization, from completely disordered random coils via molten globules and linked folded domains to mostly folded crystallizable proteins [64] in the case of biopolymers, and amorphous via self-organized structures to semicrystalline polymers in the synthetic case [53]. A reason for the attention being paid to disordered regions of proteins today is that techniques have recently been developed to analyze their structural propensities in solution by multidimensional NMR and pulsed EPR spectroscopy [64–68]. These studies of intrinsically disordered proteins (IDPs) or disordered protein regions indicate that proteins in general have a conformational ensemble of varying breadth.

As a specific example from our group showing that well-ordered proteins also can gain significant flexibility, let us consider the functional structure of human serum albumin (HSA). It is the most abundant protein in human blood plasma and serves as a transporting agent for various endogenous compounds and drug molecules [69]. Its capability to bind and transport multiple fatty acids (FA) has been studied extensively in the past. The research on HSA was severely hampered by the complexity of the protein and benefited tremendously from crystallographic high-resolution structures. Nearly 20 years ago, He and Carter reported the first crystal structure [70]. To date, a plentitude of crystal structures have been deposited in the Protein Data Bank. Even more important for understanding the binding properties of the protein, however, are the structures of complexes of HSA and transported molecules, such as fatty acids. Due to the pioneering work of Curry et al., crystal structures of various HSA–fatty acid complexes have become accessible [71]. In particular, it was found that fatty acids are distributed highly asymmetrically in the protein crystal, despite the fact that HSA itself exhibits a symmetric primary and secondary structure.

In the context of partially disordered proteins, we note that the surface exposed parts of HSA show a high degree of flexibility, which constitutes a key to the protein's

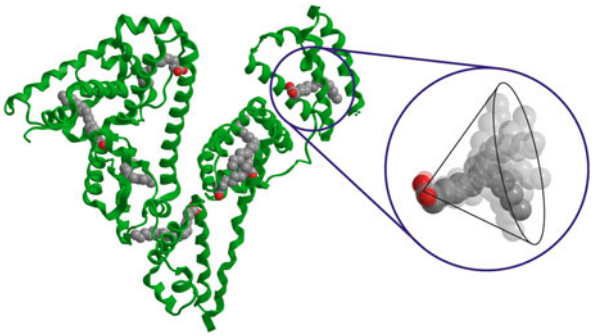

Fig. 5 Flexibility of the fatty acid binding site entry points, which results in a much more homogeneous and symmetric distribution over the protein surface than expected from the crystal structure. Only one binding site is shown for clarity. Adopted from [74]

binding versatility towards various molecules. As early as the 1950s, Karush developed a concept that accounted for conformational adaptability of the binding sites [72] and later a model was proposed that took into account the conformational entropy arising from the flexibility of the fatty acid alkyl chains [73]. As noted in Sect. 2, distances and distance distribution between spin labels on the nanometer scale can now be determined with pulsed electron–electron double resonance, DEER [20, 24]. By using spin-labeled fatty acids, it is possible to unravel the functional structure of HSA with respect to its binding of fatty acids directly from the fatty acids' point of view [74]. In this way, the distribution of the fatty acid binding sites is detected without any contribution from the complex protein itself, which is an enormous simplification. Structural information of the binding sites is obtained by determining the distance distributions between the fatty acids in frozen solution. In order to sample distances between different binding sites, fatty acids with different labeling positions can be applied. In 5-doxylstearic acid (5-DSA), the unpaired electron resides near the anchoring carboxylic acid group, in 16-DSA it is located near the end of the methylene chain. Thus, information can be retrieved separately from the anchor positions in the protein and from the entry points into the fatty acid channel formed by the protein.

The experimental distribution of 5-DSA, probing the anchoring points, nicely fits that of the crystal structure. In contrast, the distance distribution of the entry points (16-DSA) strongly deviates from that of the crystal structure and indicates that the entry points are distributed much more symmetrically and homogeneously over the protein surface than expected from the crystal structure. As depicted in Fig. 5, this leads to a picture of the functional protein structure that contains a more rigid, asymmetric inner part of the protein, while the surface of the protein shows much larger structural flexibility. These findings [74] suggest that the conformational flexibility at the periphery of HSA is a prerequisite for its function as a carrier for so many different compounds. When comparing these EPR-derived results with similar measurements on bovine serum albumin (BSA), one finds that in BSA the structural (peripheral) flexibility is far less than in HSA [75].

3.4 Dendronized Polymers

Inspired by Staudinger's vision [1], mimicking the size and eventually the function of biomacromolecules has been a dream of chemists for decades [76]. This requires not only giant molecular structures to be generated, whose dimensions are on the order of tens and even hundreds of nanometers, but also that these man-made objects should have a useful, predetermined shape. Last, but not least, at both the periphery and the interior they should contain functionalities such as recognition or catalytically active sites. Moreover, their interaction with solvents, in particular water, should be controlled and exploited in their self-organization. It is evident that successful projects in this direction will have considerable impact on both biological and materials sciences.

One approach along these lines is to incorporate building blocks such as amino acids (see Sect. 3.2), generating bioinspired polymers [77]. A full synthetic approach makes use of the enormous variety of dendrons and dendritic groups [78]; for recent reviews see [76, 79]. The structure of dendritic groups can be varied in different ways, e.g., by controlling their size by their generation, by generating amphiphilic character by incorporating hydrophobic and hydrophilic building blocks, or by varying the conformational freedom from completely rigid (polyphenylene) dendrimers [80] to highly flexible as in hyperbranched polymers [81]. Linear polymers jacketed with dendrons attached via their apex provide a conceptually simple class of dendronized polymers. For such polymers with conventional backbone, poly(styrene) or poly (methacrylate), the polymer shape can be controlled through the self-assembly of flexible dendritic side-groups and the degree of polymerization (DP) [82]. For low DP, spheres are observed, whereas for high DP, cylinders are obtained. ^{1}H and ^{13}C solid state NMR on the latter have revealed details of the organization of the dendritic groups within the supramolecular polymer [83]. The dendrons contain aromatic moieties and flexible ethylene oxide linkers (Fig. 6). In the supramolecular assembly, however, they largely lose their flexibility and exhibit dynamic order parameters S as high as 40–80%, displaying a gradient of mobility that decreases from inside out. This significant immobilization nicely demonstrates their role as structure-directing moieties displaying "edge-on" and "face-on" contacts between the ethylene units and the aromatic rings, facilitating the formation of helices (see Fig. 6).

The shape of macromolecular objects can also be changed by external stimuli [84]. For instance, thermoresponsive polymeric materials are of great interest owing to their potential use in fields such as actuation, drug delivery, and surface modification [85]. Ever since the discovery by Wu and coworkers of the coil–globule transition of single poly(*N*-isopropylacrylamide) (PNiPAAm) chains near the lower critical solution temperature (LCST) [86], the collapse mechanism and the formation of stable mesoglobules have been intense topics of research [84, 87]. Despite these efforts, a molecular-scale picture of what happens when thermoresponsive polymers start to dehydrate at a certain temperature, subsequently collapse, and then assemble to mesoglobules, did not exist. This absence severely hampered rational materials design. Dendronized polymers with amphiphilic dendritic groups based on

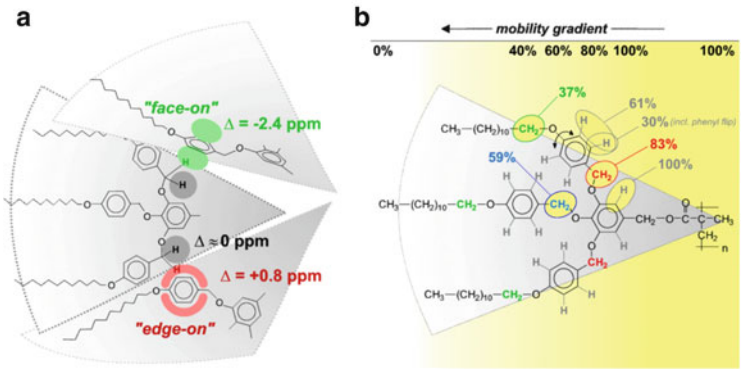

Fig. 6 Structure and dynamics of directing dendrons in cylindrical supramolecular macromolecules. (**a**) Local packing allows the formation of helices. (**b**) Restricted motion, as indicated by high dynamic order parameters, with a mobility gradient inside-out. Adopted from [83]

oligoethyleneglycol (OEG) helped to shed more light on the phase separation because they exhibit fast and fully reversible as well as particularly sharp transitions, as observed in turbidity measurements [88]. These dendronized polymers with terminal ethoxy groups are soluble in water. Their LCSTs lie in a physiologically interesting temperature range between 30 and 36°C and mainly depend on the periphery of the dendrons.

There are indications, however, that such thermal responses proceed by via the formation of structural inhomogeneities of variable lifetimes on the nanometer scale that are still poorly understood. Indeed, this topic has been identified as one of the major challenges of current research in the macromolecular sciences [89]. The structure and lifetime of these local inhomogeneities will obviously influence the aspired function, for instance drug delivery. Magnetic resonance techniques, as intrinsically local methods, are particularly suited to probe structural inhomogeneities of functional macromolecules in general [14, 21] For instance, with multidimensional NMR, the lifetime of dynamic heterogeneities in polymer melts in the vicinity of the glass transition was identified as early as 1991 [90].

A particularly simple way of studying the molecular environment of thermoresponsive dendronized polymers, which undergo a thermal transition, utilizes conventional continuous wave (CW) EPR spectroscopy on nitroxide radicals, as paramagnetic tracer molecules [21]. As noted above, such spin probes are sensitive to the local viscosity, which will give rise to changes in the rotational correlation time and to the local polarity/hydrophilicity [21, 22]. The latter affects the electronic structure of the radical and changes the spectral parameters, specifically the g-factor and the hyperfine coupling constant to ^{14}N. The amphiphilic radical 2,2,6,6-tetramethylpiperidine-1-oxyl (TEMPO) is especially suited to sample both hydrophobic and hydrophilic regions and also mimics a small molecule to be delivered by the dendronized polymer.

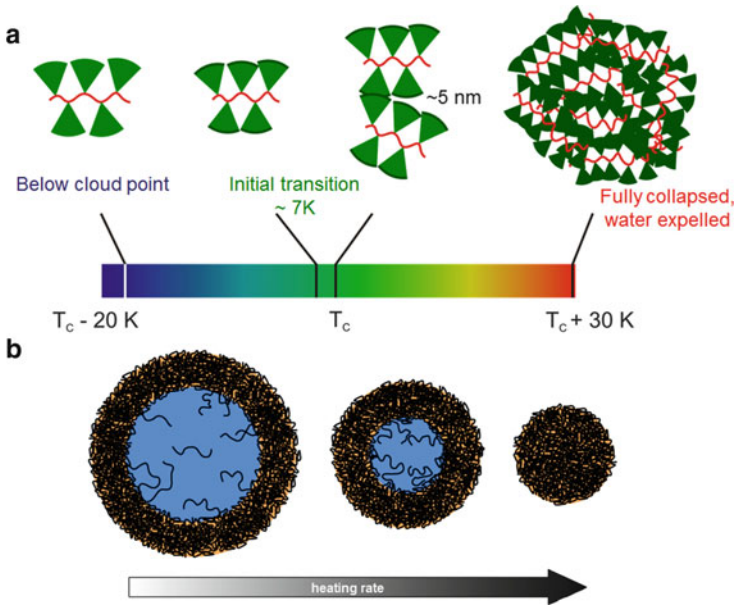

Fig. 7 (**a**) Thermal collapse of dendronized polymers, as deduced from EPR spectroscopy of admixed spin probes [91]. (**b**) Skin barrier effect in mesoglobules of different sizes [91]

The results of such a study [91] are depicted in Fig. 7a. When the temperature is raised above the transition temperature T_C, the aggregation of the complete polymer sample is triggered by dynamic structural inhomogeneities of a few nanometers. In this temperature regime the spin probes exchange between large hydrophilic and small hydrophobic regions. Although macroscopic turbidity measurements suggest a sharp phase transition of the polymer, EPR spectroscopy reveals that the dehydration of the polymer chains proceeds over a temperature interval of at least 30°C. It cannot be described by a single de-swelling process that would be expected for a thermodynamic phase transition. Rather, the dehydration should be viewed as a molecularly controlled nonequilibrium process that takes place in two steps. The local heterogeneities grow in size, and polymer chain fluctuations slow down. Within ~7°C above T_C, the majority of the dehydration is complete and percolation for the fraction and volume of hydrophobic regions is reached. Heating the samples to even higher temperatures leads to additional losses of residual water from the collapsed system. Although the aggregation temperature mainly depends on the periphery of the dendrons, the dehydration process itself is sensitive to the inner core, with the dehydration efficiency being strongly related to the hydrophobicity of the core.

In a subsequent study [92], differences in the EPR spectra in dependence of the heating rate, the chemical nature of the dendritic substructure of the polymer, and the concentration were interpreted to indicate the formation of a dense polymeric layer at the periphery of the mesoglobule (Fig. 7b). This skin barrier [85] is formed in a

narrow temperature range of ~4 K above T_C and prohibits the release of molecules that are incorporated in the polymer aggregate. In large mesoglobules, formed at low heating rates and at high polymer concentrations, a considerable amount of water is entrapped and a microphase separates from the collapsed polymer chains at high temperatures. This results in aggregates possessing an aqueous core and a corona consisting of collapsed polymer chains. Fast heating rates, low polymer concentrations, and hydrophobic subunits in the polymer make the entrapment of water less favorable and lead to a higher degree of vitrification. This has obvious consequences for the design and use of thermoresponsive polymeric systems in the fast growing field of drug delivery.

Following A. D. Schlüter's question of "whether one can create a molecular object, i.e., a molecular system that does not respond to its surrounding, by making a polymer thicker and thicker" [93], shape-persistent dendronized polymers in solution were studied by advanced pulse EPR methods. As expected, DEER spectroscopy yields the size (thickness) of different generations of charged cylindrical dendronized polymers in solution [94]. Moreover, a combination of CW EPR and a modified isotopolog-specific DEER variant provides a better understanding of how amphiphilic molecules can be loaded into and released upon external stimulation from these thick polymers [95].

4 Functional Materials

Macromolecular and supramolecular systems are becoming increasingly important as functional materials in various applications, e.g., ion conductors [96], sensors [97], and organic electronics [98]. In all cases, magnetic resonance provides unprecedented details of structure and dynamics [99–104]. Moreover, applications for synthetic polymers in medicine are emerging [105]. Research at the interface of polymer chemistry and the biomedical sciences has given rise to the first nanosized (5–100 nm) polymer-based pharmaceuticals, the "polymer therapeutics." Polymer therapeutics include rationally designed macromolecular drugs, polymer–drug and polymer–protein conjugates, polymeric micelles containing covalently bound drug, and polyplexes for DNA delivery. Another important route for generating nanoparticles and controlling their interaction with cells is provided by miniemulsion polymerization [106], which can also be used to encapsulate, e.g., magnetic contrast agents for magnetic resonance imaging (MRI) [107].

4.1 Elastin-Like Polypeptides and Drug Delivery

Drug release can, of course, also be realized using building blocks from nature. In this respect, elastin-like polypeptides (ELPs) are particularly interesting [51]. ELPs are genetically encoded polymers composed of repeats of the amino acid VPGXG

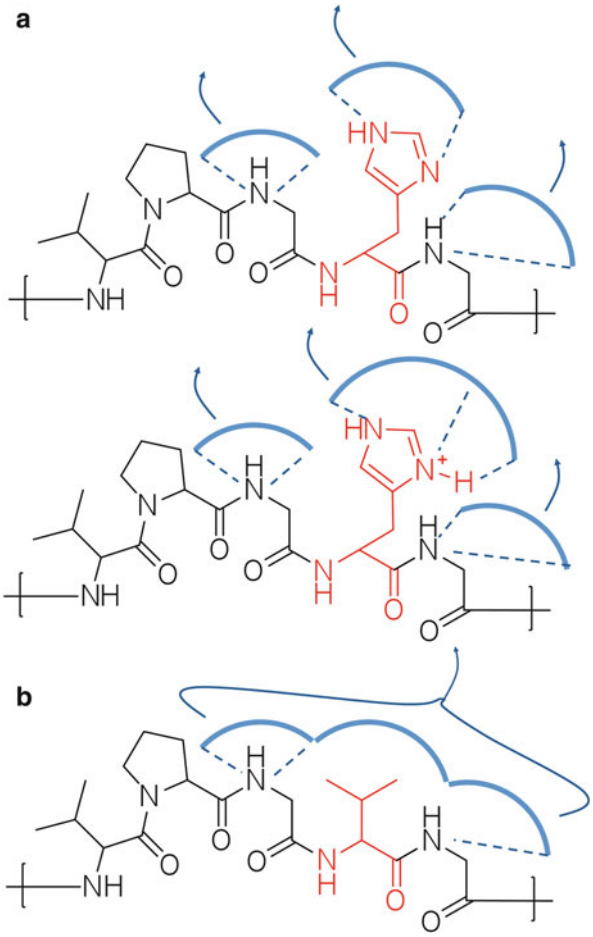

Fig. 8 Putative hydration for ELPs with (**a**) protic guest-residue side chains and (**b**) aprotic guest-residue side chains. (**a**) The hydration layer of the protic guest-residue side chain is individually stabilized by H-bonds and can vanish independently (decoupled) from backbone hydration layers. When the His residues are charged (*bottom*) the individual (decoupled) side chain hydration layers are even more stable than in the charge neutral analog (*top*). The higher stability is schematically depicted as larger hydration shell and larger number of H-bonds. (**b**) The hydration layer of the guest-residue side chain is stabilized via coupling to neighboring backbone hydration layers and, hence, dehydration takes place cooperatively. Adopted from [108]

motif found in tropoelastin (X being the so-called guest residue, which can be any amino acid except proline). Their LCST phase behavior at the molecular level can be fine-tuned by the choice of the guest residue, their chain length, and by the cosolutes [108]. This makes them excellent candidates for studying fundamental aspects of intrinsically disordered polypeptides on the one hand and thermoresponsive polymers, on the other hand.

In a recent study using simple CW EPR spectroscopy [22], new light could be shed on the dehydration mechanism in LCST-polypeptides [109]. It was shown that hydrophilic (backbone) and hydrophobic (side chain) hydration layers of ELPs can exist in a coupled state or a decoupled state (Fig. 8). The decoupled hydration state consists of hydrophobic and hydrophilic hydration layers that respond independently to temperature whereas the coupled hydration state is characterized by a common, cooperative dehydration of both hydration layers. The authors could show that the primary sequence of an ELP can be tuned to exhibit either of the hydration layer coupling modes. Charged side chains lead to decoupling, whereas strongly hydrophobic side chains trigger stronger interaction between hydrophilic and hydrophobic hydration, leading to coupling of both layers. These results indicate that ELPs are the first identified class of polymers that exhibit a first-order inverse phase transition on nanoscopic length scales. These findings are important for the understanding and further use of ELPs in applications such as drug delivery and may also provide insights into the role of hydration layers in governing the structure–function relationship of intrinsically disordered proteins, as discussed above.

4.2 Columnar Stacks

Columnar stacks are the structure-determining feature of discotic liquid crystals (DLCs) [24]. As noted in the "Introduction", the disc-shaped aromatic core units rotate around the column axis, which can conveniently be studied by NMR via ^{1}H–^{13}C dipole–dipole or ^{2}H quadrupole coupling. Moreover, imperfections of the parallel packing within the column lead to a reduction in the dynamic order S to values below 0.5. Such disorder was indeed observed early on for the extended hexabenzocoronene (HBC) units with alkyl chains attached, whereas the smaller triphenylene moieties lead to much narrower DLC phase ranges, but are much better packed [110]. In fact, the high charge-carrier mobility in a highly ordered helical columnar structure derived from a triphenylene derivative [111] generated a remarkable interest in the semiconducting, photoconducting, and other electronic properties of columnar liquid crystal materials. By incorporating a phenylene ring between the HBC core and the alkyl chain, the order within the column of HBC could be greatly improved [112] and, together with perylenediimide (PDI), was used to generate highly efficient self-organized thin films for organic photovoltaics [113].

Indeed, PDI derivatives are attractive in all-organic photovoltaic solar cells and field-effect transistors. These applications rely on the high charge carrier mobilities that made PDI the best n-type semiconductors available to date [113]. PDIs have an elongated shape, and can therefore display considerable dynamics even in the frozen, crystal-like state. This was observed in a triethyleneglycol (TEG)-substituted PDI [114]. From X-ray scattering, we found that the PDI building blocks assemble into columns arranged in a hexagonal unit cell with a lattice parameter of 2.23 nm. The meridional reflections in the wide-angle region are assigned to the π-stacking distance of 0.34 nm between individual molecules in the stacks. Additional weak and diffuse off-meridional reflections show a d-spacing of 0.70 nm, i.e., twice the simple

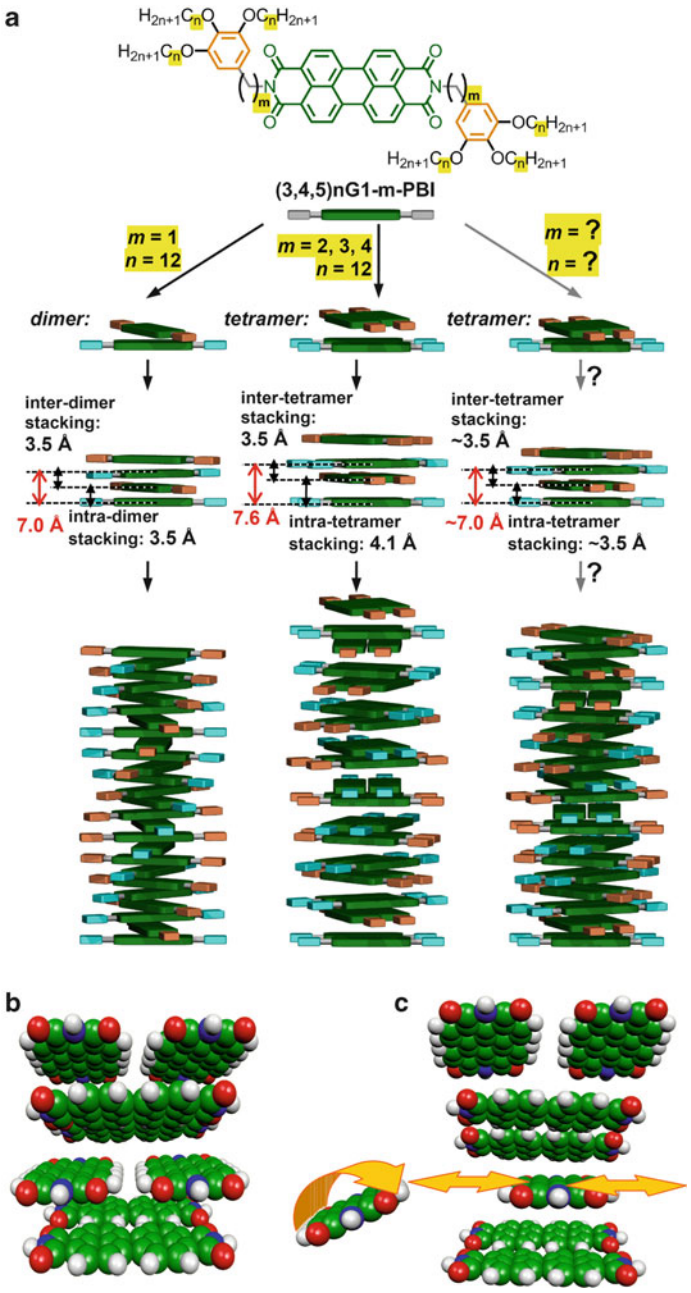

Fig. 9 (**a**) Packing of dendronized PBI with equal intra- and interdimer stacking (*left* and *right*, respectively) of 0.35 nm, but larger intradimer packing of 0.41 nm due to nonequilibrium disorder (*middle*). (**b**) Tetramer motif stacking into columns. (**c**) Molecular reorganization: one PBI leaves the columns, flips over, and enters a column again. Adopted from [117]

π-stacking, indicating correlations of adjacent TEG-PDI molecules perpendicular to each other. The dynamics of these systems was studied by different solid state NMR techniques. These showed that TEG-PDI in its frozen state performs angular fluctuations with amplitudes up to ±40°, reflecting the rather fragile packing of the elongated PDI units perpendicular to each other. In the liquid crystal phase, additional motional averaging in the NMR spectra is observed. The easiest motional process consistent with the observed averaging involves cooperative rotation of the PDI molecules by 90° around the column axis. Thus, whereas the restricted angular fluctuations in the solid phase can be considered as local processes, the increased dynamics in the liquid crystal phase must be highly cooperative in nature. Such cooperative dynamic modes are, of course, particularly important in processing such systems to align the columns on surfaces [115].

Moreover, slow molecular dynamics and very slow phase transformation [116] hamper the formation of the equilibrium phases of DLCs and the different packing in equilibrium and nonequilibrium phases can have pronounced effects on the charge carrier mobilities. This was studied in detail in perylene bis(diimide)s (PBIs) functionalized with dendritic groups [117, 118]. These dendronized PBIs self-assemble into complex helical columns generated from tetramers containing a pair of two molecules arranged side-by-side and another pair in the next stratum of the column, turned upside-down and rotated around the column axis at an intratetramer angle that is different from that of the intertetramer angle (Fig. 9).

In most cases, the intratetramer stacking distance in this column is 0. 41 nm, while the intertetramer distance is 0. 35 nm The architecture of this complex helical column, the structure of its 3D periodic array, and its kinetically controlled self-organization with such a long intratetramer distance are not ideal for the design of supramolecular structures with high charge-carrier mobility. In fact, the mobility of electrons is only moderate. However, in some cases, heating above 100°C in the liquid crystal phase optimizes the packing and results in shorter intratetramer distances and much higher charge mobilities [117, 118]. This is accompanied by substantial narrowing of the ^{1}H NMR lines. Computer simulation showed that this narrowing of the NMR spectra indicates a complex reorganization mechanism, whereby the PBI molecules leave the supramolecular column, flip over, and reenter a column at a later time (Fig. 9b, c).

4.3 Pi-Conjugated Macromolecules for Organic Electronics

Likewise, polymers with extended π-conjugation and low band gaps are of broad scientific interest because of their promising applications as semiconductors in organic electronic devices. Examples include organic photovoltaic (OPV) cells, organic field-effect transistors (OFETs), and organic light-emitting diodes (OLEDs) with optimized properties toward light harvesting, charge-carrier mobility, and light emission, respectively [119–121]. Such polymers with lamellar π-stacks are often semicrystalline [53], i.e., they exhibit phase separation with regions of high and low

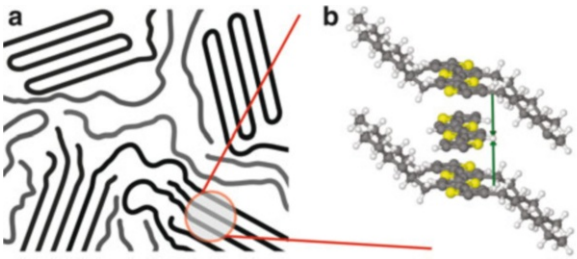

Fig. 10 (**a**) Semicrystalline polymer with regions of high (*black*) and low (*grey*) order. (**b**) View along the stacked P3HT structure, illustrating the alternating packing of P3HT polymer chains. For details see [122]

order. The specific organization of the macromolecules depends on the processing conditions. X-ray diffraction (XRD), which is well established in structure elucidation, requires high order, like that of single crystals, if atomic resolution is sought. From a fiber diagram, often employed in polymer science [53], only information about the relative assembly on a crystallographic lattice, or chain-to-chain and π–π stacking distances, can be derived. Thus, a "multi-technique" approach is required to fully elucidate such structures.

Along these lines, we recently introduced a new systematic strategy for revealing the local packing in such polymer systems [122]. Our strategy makes use of the space group (i.e., one of the first steps in a conventional approach to solve a crystal structure), distance constraints from ^{1}H DQ NMR, and chemical shifts. These experimental results are unified by quantum-chemical calculations, enabling the verification of specific packing models in silico and quantification of π-stacking effects. In order to illustrate the potential of our strategy, we chose poly(3-hexyl-thiophene) (P3HT) as a prominent example. It is one of the most frequently studied semiconducting polymers because of its widespread applications in organic electronic devices, resulting from its facile processability, high charge-carrier mobility (up to 0.1 $Vcm^2\ s^{-1}$), and environmental stability (see Fig. 10) [123].

Our approach can be compared with that employed for determining the solution structures of biomacromolecules by NMR through distance constraints (nuclear Overhauser effect, NOE) and chemical shifts [11, 12]. This, however, requires a large number of NOE constraints, whereas in a crystalline solid, the periodicity described by the space group gives access to the full 3D structure from only a few constraints. Thus, our strategy, which we propose to term "multi-technique crystallography," can be applied in general to provide quantitative insights into the packing of semicrystalline polymers with specific intermolecular packing features, such as hydrogen bonds or stacking of aromatic moieties. In fact, similar approaches, often termed "NMR crystallography" [124] are increasingly applied in unraveling the structures of pharmaceuticals [125–127] or supramolecular systems in general [128, 129].

In order to achieve high charge-carrier mobility, donor and acceptor groups can be mixed, as was done in supramolecular stacks with or without a polymer backbone [130]. Such groups can also be incorporated into a copolymer consisting of an alternating arrangement of cyclopentadithiophene (CDT) as a donor and benzothiadiazole (BTZ) as an acceptor unit, as reported recently [131] (see Fig. 11).

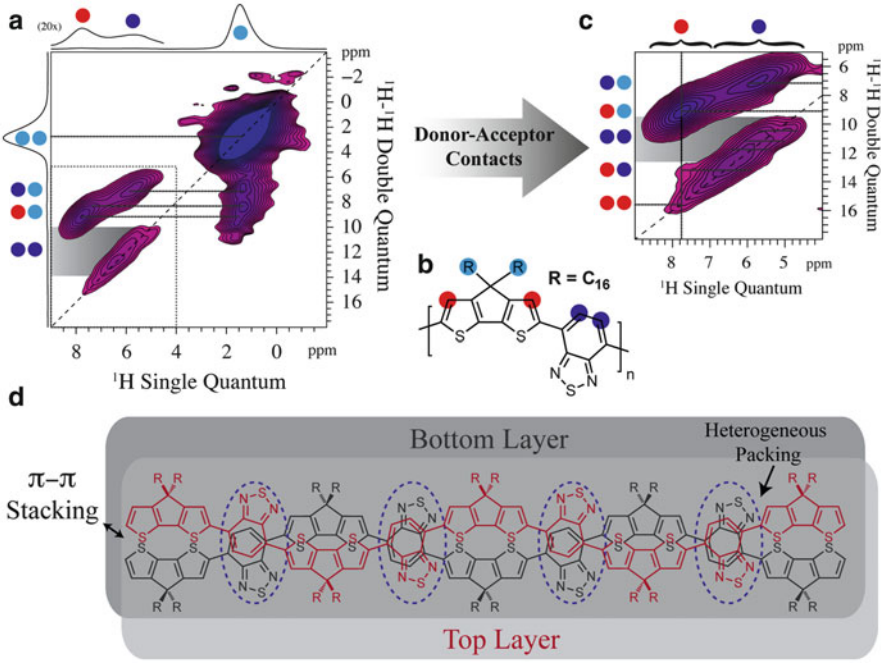

Fig. 11 Local packing and organization of the donor–acceptor groups in a CDT-PTZ copolymer. (**a**) Two-dimensional contour plot of the ^{1}H–^{1}H DQ NMR spectrum. (**b**) Color scheme used for assignments. (**c**) Expansion of the backbone region showing the contacts between donor and acceptor groups. (**d**) Local packing of donor–acceptor groups in two neighboring CDT-BTZ copolymer chains. Adopted from [131]

Field-effect transistor (FET) hole mobilities exceeding 3 V cm^2 s^{-1} have been obtained and these were shown to be strongly sensitive to the molecular weight of the hexadecyl-substituted copolymers. Solid state NMR was used to assess the supramolecular organization of the conjugated chains. The ^{1}H 2D DQ NMR spectra clearly revealed the relevant packing contacts, confirming the expected π–π stacking for the polymer backbone. The packing of the donor and the acceptor groups, however, was found to be more delicate. Donor–acceptor groups are π–π stacked in a lamellar fashion and these groups are ordered in an alternating way, as shown in Fig. 11d. Thereby, the acceptor groups in one layer are located on top of the acceptor groups in adjacent layers; however, they are not always in the exact same position, leading to heterogeneous packing. This model derived from NMR is consistent with the findings of X-ray scattering. It also allows for optimal packing of the side chains, which in the case of long and bulky alkyl chains (C_{16}) should be advantageous in order to avoid steric clash. Conclusively, solid state NMR does not reveal a donor–acceptor overlap within 0.4 nm. Thus, strikingly, donor–acceptor interaction between the neighboring CDT and BTZ groups located at adjacent chains apparently contributes

little, if anything, to the observed improvement in charge-carrier mobility. NMR rather unravels the complexity of this remarkable CDT-BTZ copolymer system.

This result was confirmed by molecular modeling of this system [132], which showed that the longitudinal displacement of the conjugated backbones by 1–2 Å changes the electronic coupling mediating hole hopping by over one order of magnitude. Interestingly, these subtle structural changes have clear fingerprints in X-ray diffraction patterns and ^{1}H NMR chemical shifts, which allow refining the structural parameters down to the molecular scale. From this study, it was concluded that the unprecedented hole carrier mobilities observed in fibers of the CDT-BTZ copolymers arise from a close packing of the polymer chains into a close-to-registry assembly, providing optimal wavefunction overlap, together with the intrinsically higher electronic bandwidth for charge motion along the chains. This arrangement is primarily triggered by van der Waals interactions between the long, linear alkyl chains and not by electrostatic donor–acceptor interactions. This rather unexpected result emphasizes how important the detailed information on the packing provided by a multi-technique approach including solid state NMR is to obtain unbiased structural details, which are needed to optimize the structure for specific applications.

5 Conclusion

Following the pioneering work of Hermann Staudinger [1], advances in the synthesis, characterization, and understanding of macromolecular and supramolecular systems have led to an enormous variety and complexity in the field of polymer science [89]. The traditional separation in terms of structure versus dynamics, crystalline versus amorphous, or experiment versus theory is increasingly being overcome. As far as characterization of such materials is concerned, no experimental or theoretical/simulation approach alone can provide full information. Instead, a combination of techniques is called for and conclusions should be backed by results provided by as many complementary methods as possible [27]. As demonstrated in this contribution, the information provided by NMR and EPR is often indispensable and unique. Combining scattering or MR spectroscopy with computer simulation is well established today in the study of the structure and dynamics of biomacromolecules and provides new insight in the emerging field of partially disordered proteins [64]. The examples described here show the power of such an approach involving the combination of spectroscopy, scattering, and computer simulation in the supramolecular field.

Last, but not least, the development of NMR spectroscopy is far from complete [133]. In particular, in order to meet the ever-increasing demands of miniaturization, the sensitivity of NMR spectroscopy has to be increased substantially and several approaches in response to that challenge are underway [134–137], down to the detection of single spins [138]. Remarkably, in this area the combination of

NMR and EPR called "dynamic nuclear polarization" is very advanced and has already been successfully applied in magnetic resonance imaging [139].

Acknowledgments This tribute to Hermann Staudinger is based on my work at the Max Planck Institute for Polymer Research in Mainz for more than 25 years. It has provided me with a unique scientific environment, in which new ideas and approaches prospered. It gives me great pleasure to thank my colleagues and coworkers for all their contributions. Special thanks are due to Dariush Hinderberger for his suggestions concerning the EPR studies described in this chapter.

References

1. Nobelprize.org (1964) Hermann Staudinger – Nobel lecture: macromolecular chemistry. In: Nobel lectures, chemistry 1942–1962. Elsevier, Amsterdam. http://www.nobelprize.org/nobel_prizes/chemistry/laureates/1953/staudinger-lecture.pdf
2. Zavoisky E (1945) J Phys USSR 9:211
3. Purcell EM, Torrey HC, Pound RV (1946) Phys Rev 69:37
4. Bloch F, Hansen WW, Packard M (1946) Phys Rev 69:127
5. Zambelli A, Segre AL, Farina M, Natta G (1967) Makromol Chem 110:1
6. Tonelli AE, Schilling FC (1981) Acc Chem Res 14:233
7. Ferry JD (1980) Viscoelastic properties of polymers, 3rd edn. Wiley, Chichester
8. Matyjaszewski K, Möller M (eds) (2012) Polymer science: a comprehensive reference. Elsevier, Amsterdam
9. Slichter WP (1959) Makromol Chem 34:67
10. Spiess HW (1983) Colloid Polym Sci 261:193
11. Ernst RR, Bodenhausen G, Wokaun A (1987) Principles of nuclear magnetic resonance in one and two dimensions. Clarendon, Oxford
12. Wüthrich K (2003) Angew Chem Int Ed 42:3340
13. Hong M, Schmidt-Rohr K (2013) Acc Chem Res 46:2154
14. Schmidt-Rohr K, Spiess HW (1994) Multidimensional solid-state NMR and polymers. Academic, London
15. Lehn JM (1988) Angew Chem Int Ed 27:89
16. Brown SP, Spiess HW (2001) Chem Rev 101:4125
17. Abragam A (1961) The principles of nuclear magnetism. Clarendon, Oxford
18. Abragam A, Bleany B (1970) Electron paramagnetic resonance of transition ions. Oxford University Press, Oxford
19. Schweiger A, Jeschke G (2001) Principles of pulse paramagnetic resonance. Oxford University Press, Oxford
20. Jeschke G (2012) Annu Rev Phys Chem 62:419
21. Schlick S (2006) Advanced ESR methods in polymer research. Wiley, Hoboken
22. Hinderberger D (2012) Top Curr Chem 321:67
23. Höfer P, Grupp A, Nebenführ H, Mehring M (1986) Chem Phys Lett 132:279
24. Pannier M, Veit S, Godt A, Jeschke G, Spiess HW (2000) J Magn Resonance 142:331
25. Hubbell WL, Cafiso DS, Altenbach C (2000) Nature Struct Biol 7:735
26. Warren BE (1969) X-ray diffraction. Addison-Wesley, Reading
27. Spiess HW (2010) Macromolecules 43:5479
28. Brown SP (2009) Macromol Rap Comm 30:688
29. Saalwächter K, Spiess HW (2012) Polymer science: a comprehensive reference, vol 2. Elsevier, Amsterdam, p 185. doi:10.1016/B978-0-444-53349-4.00025-X
30. Hansen MR, Graf R, Spiess HW (2013) Acc Chem Res 46:1996
31. Sebastiani D (2006) ChemPhysChem 7:164

32. Müllen K, Rabe JP (2008) Acc Chem Res 41:511
33. Hansen MR, Graf R, Sekharan S, Sebastiani D (2009) J Am Chem Soc 131:5251
34. Demus D, Goodby J, Gray G, Spiess HW, Vill V (1998) Handbook of liquid crystals. Wiley-VCH, Weinheim
35. Hansen MR, Feng X, Macho V, Müllen K, Spiess HW, Floudas G (2011) Phys Rev Lett 107:257801
36. Berliner LJ (1979) Spin labeling theory and applications. Academic, New York
37. Goldman SA, Bruno GV, Polnaszek CF, Freed JH (1972) J Chem Phys 56:716
38. Spiess HW (2004) J Poly Sci A 42:5031
39. Mierzwa M, Floudas G, Neidhöfer M, Graf R, Spiess HW, Meyer WH, Wegner G (2002) J Chem Phys 117:6289
40. Beiner M (2001) Macromol Rapid Commun 22:869
41. Wind M, Graf R, Heuer A, Spiess HW (2003) Phys Rev Lett 91:155702
42. Wind M, Graf R, Heuer A, Renker S, Spiess HW, Steffen W (2005) J Chem Phys 122:014906
43. Wind M, Graf R, Heuer A, Renker S, Spiess HW (2005) Macromol Chem Phys 206:142
44. Friedrichs C, Emmerling S, Kircher G, Graf R, Spiess HW (2013) J Chem Phys 138:12A503
45. de Gennes PG (1975) J de Physique 36:1199
46. Adams CH, Brereton MG, Hutchings LR, Klein PG, McLeish TCB, Richards RW, Ries ME (2000) Macromolecules 33:7101
47. Lo Verso F, Yelash L, Binder K (2013) Macromolecules 46:4716
48. Saalwächter K (2007) Prog Nucl Mag Res Spec 51:1
49. Yao YF, Graf R, Spiess HW, Rastogi S, Lippits DR (2007) Phys Rev E 76:060801(R)
50. Klok HA, Lecommandoux S (2006) Adv Polym Sci 202:75
51. McDaniel JR, Callahan DJ, Chilkoti A (2010) Adv Drug Delivery Rev 62:1456
52. Tycko R (2001) Ann Rev Phys Chem 52:575
53. Strobl G (2007) The physics of polymers: concepts for understanding their structures and behavior, 3rd edn. Springer, Heidelberg
54. Stockmayer WH (1967) Pure Appl Chem 15:539
55. Floudas G (2004) Progr Polym Sci 29:1143
56. Floudas G, Spiess HW (2009) Macromol Rapid Commun 30:278
57. Aliferis T, Iatrou H, Hadjichristidis N (2004) Biomacromolecules 5:1653
58. Gitsas A, Floudas G, Mondeshki M, Lieberwirth I, Spiess HW, Iatrou H, Hadjichristidis N, Hirao A (2010) Macromolecules 43:1874
59. Graf R, Spiess HW, Floudas G, Butt HJ, Gkikas M, Iatrou H (2012) Macromolecules 45:9326
60. Ringsdorf H (2004) Angew Chem Int Ed 43:1064
61. Ringsdorf H, Schlarb B, Venzmer J (1988) Angew Chem Int Ed 27:113
62. Ober CK, Wegner G (1997) Adv Mat 9:17
63. Worldwide Protein Data Bank http://www.wwpdb.org/
64. Dyson HJ, Wright PE (2005) Nat Rev Mol Cell Biol 6:197
65. Konrat R (2010) Structure 18:416
66. Ozenne V, Schneider R, Yao MX, Huang JR, Salmon L, Zweckstetter M, Jensen MR, Blackledge M (2012) J Am Chem Soc 134:15138
67. Drescher M (2012) Top Curr Chem 321:91
68. Kurzbach D, Platzer G, Schwarz T, Henen MA, Konrat R, Hinderberger D (2013) Biochemistry 52:5167 doi:10.1021/bi400502c
69. Peters T (1995) All about albumin: biochemistry, genetics and medical applications. Academic, San Diego
70. He XM, Carter DC (1992) Nature 358:209
71. Curry S, Mandelkow H, Brick P, Franks NP (1998) Nature Struc Biol 5:827
72. Karush F (1950) J Am Chem Soc 72:2705
73. Laiken N, Nemethy G (1971) Biochemistry 10:2101
74. Junk MJN, Spiess HW, Hinderberger D (2010) Angew Chem Int Ed 49:8755
75. Akdogan A, Reichenwallner J, Hinderberger D (2012) PLoS ONE 7:e45681

76. Schlüter AD (2005) Top Curr Chem 245:151
77. Kricheldorf HR (2006) Angew Chem Int Ed 45:5752
78. Fréchet JMJ, Tomalia DA (2001) Dendrimers and other dendritic polymers. Wiley-VCH, Chichester
79. Rosen BM, Wilson CJ, Wilson DA, Peterca M, Imam MR, Percec V (2009) Chem Rev 109:6275
80. Morgenroth F, Berresheim AJ, Wagner M, Müllen, K (1998) Chem Commun 1998(10):1139
81. Sunder A, Hanselmann R, Frey H, Mülhaupt R (1999) Macromolecules 32:4240
82. Percec V, Ahn CH, Ungar G, Yeardley DJP, Möller M, Sheiko SS (1998) Nature 391:161
83. Rapp A, Schnell I, Sebastiani D, Brown SP, Percec V, Spiess HW (2003) J Am Chem Soc 125:13284
84. Gil ES, Hudson SM (2004) Prog Polym Sci 29:1173
85. Schild HG (1992) Prog Polym Sci 17:163
86. Wu C, Zhou SQ (1995) Macromolecules 28:5388
87. Keerl M, Pedersen JS, Richtering W (2009) J Am Chem Soc 131:3093
88. Li W, Zhang AA, Schlüter AD (2008) Chem Commun 2008(43):5523
89. Ober CK, Cheng SZD, Hammond PT, Muthukumar M, Reichmanis E, Wooley KL, Lodge TP (2009) Macromolecules 42:465
90. Schmidt-Rohr K, Spiess HW (1991) Phys Rev Lett 66:3020
91. Junk MJN, Li W, Schlüter AD, Wegner G, Spiess HW, Zhang A, Hinderberger D (2010) Angew Chem Int Ed 49:5683
92. Junk MJN, Li W, Schlüter AD, Wegner G, Spiess HW, Zhang A, Hinderberger D (2011) J Am Chem Soc 133:10832
93. Zhang B, Wepf R, Fischer K, Schmidt M, Besse S, Lindner P, King BT, Sigel R, Schurtenberger P, Talmon Y, Ding Y, Kroeger M, Halperin A, Schlüter AD (2011) Angew Chem Int Ed 50:737
94. Kurzbach D, Kattnig DR, Zhang B, Schlüter AD, Hinderberger D (2011) J Phys Chem Lett 2:1583
95. Kurzbach D, Kattnig DR, Zhang B, Schlüter AD, Hinderberger D (2012) Chem Sci 3:2550
96. Kreuer KD, Paddison SJ, Spohr E, Schuster M (2004) Chem Rev 104:4637
97. McQuade TD, Pullen AE, Swager TM (2000) Chem Rev 104:4637
98. Dimitrakopoulos CD, Malenfant PRL (2002) Adv Mat 14:99
99. Grey CP, Dupre N (2004) Chem Rev 100:2537
100. Akbey U, Granados-Focil S, Coughlin EB, Graf R, Spiess HW (2009) J Phys Chem B 113:9151
101. Tolbert SH, Firouzi A, Stucky GD, Chmelka BF (1997) Science 278:264
102. Pawsey S, McCormick M, De Paul S, Graf R, Lee YS, Reven L, Spiess HW (2003) J Am Chem Soc 125:4174
103. Pascui OF, Lohwasser R, Sommer M, Thelakkat M, Thurn-Albrecht T, Saalwächter K (2010) Macromolecules 43:9401
104. Brown SP, Schnell I, Brand JD, Müllen K, Spiess HW (1999) J Am Chem Soc 121:6712
105. Duncan R (2003) Nat Rev Drug Disc 2:347
106. Landfester K (2009) Angew Chem Int Ed 48:4488
107. Mailänder V, Landfester K (2009) Biochemistry 10:2379
108. MacKay JA, Callahan DJ, Fitzgerald KN, Chilkoti A (2010) Biomacromolecules 11:2873
109. Kurzbach D, Hassouneh W, McDaniel JR, Jaumann EA, Chilkoti A, Hinderberger D (2013) J Am Chem Soc 135:11299. doi:10.1021/ja4047872
110. Herwig P, Kayser CW, Müllen K, Spiess HW (1996) Adv Mater 8:510
111. Adam D, Schumacher P, Simmerer J, Häussling L, Siemensmeyer K, Etzbach KH, Ringsdorf H, Haarer D (1994) Nature 371:141
112. Fechtenkötter A, Saalwächter K, Harbison MA, Müllen K, Spiess HW (1999) Angew Chem Int Ed 38(20):3039

113. Schmidt-Mende L, Fechtenkötter A, Müllen K, Moons E, Friend RH, MacKenzie JD (2001) Science 293:1119
114. Hansen MR, Schnitzler T, Pisula W, Graf R, Müllen K, Spiess HW (2009) Angew Chem Int Ed 48:4621
115. Feng XP, Pisula W, Müllen K (2007) J Am Chem Soc 129:14116
116. Tasios N, Grigoriadis C, Hansen MR, Wonneberger H, Li C, Spiess HW, Müllen K, Floudas G (2010) J Am Chem Soc 132:7478
117. Percec V, Hudson SD, Peterca M, Leowanawat P, Aqad E, Graf R, Spiess HW, Zeng X, Ungar G, Heiney PA (2011) J Am Chem Soc 133:18479
118. Percec V, Sun HJ, Leowanawat P, Peterca M, Graf R, Spiess HW, Zeng X, Ungar G, Heiney PA (2013) J Am Chem Soc 135:4129
119. Burroughes JH, Bradley DDC, Brown AR, Marks RN, Mackay K, Friend RH, Burns PL, Holmes AB (1990) Nature 347:539
120. Thompson BC, Frèchet JMJ (2008) Angew Chem Int Ed 47:58
121. Blom PWM, Mihailetchi VD, Koster LJA, Markov DE (2007) Adv Mat 19:1551
122. Dudenko D, Kiersnowski A, Shu J, Pisula W, Sebastiani D, Spiess HW, Hansen MR (2012) Angew Chem Int Ed 51:11068
123. Sirringhaus H, Brown PJ, Friend RH, Nielsen MM, Bechgaard K, Langeveld-Voss BMW, Spiering AJH, Janssen RAJ, Meijer EW, Herwig P, de Leeuw DM (1999) Nature 401:685
124. Harris RK, Wasylishen RE, Duer MJ (2009) NMR crystallography. Wiley-VCH, Weinheim
125. Griffin JM, Martin DR, Brown SP (2007) Angew Chem Int Ed 46:8036
126. Mafra L, Santos SM, Siegel R, Alves I, Almeida Paz FA, Dudenko D, Spiess HW (2012) J Am Chem Soc 134:71
127. Baias M, Widdifield CM, Dumez JN, Thompson HPG, Cooper TG, Salager E, Bassil S, Stein RS, Lesage A, Day GM, Emsley L (2013) Phys Chem Chem Phys 15:8069
128. Metzroth T, Hoffmann A, Martin-Rapun R, Smulders MMJ, Pieterse K, Palmans ARA, Vekemans JAJM, Meijer EW, Spiess HW, Gauss J (2011) Chem Sci 2:69
129. Fritzsche M, Bohle A, Dudenko D, Baumeister U, Sebastiani D, Richardt G, Spiess HW, Hansen MR, Hoeger S (2011) Angew Chem Int Ed 50:3030
130. Percec V, Glodde M, Bera TK, Miura Y, Shiyanovskaya I, Singer KD, Balagurusamy VSK, Heiney PA, Schnell I, Rapp A, Spiess HW, Hudson SD, Duan H (2002) Nature 419:384
131. Tsao HN, Cho DM, Park I, Hansen MR, Mavrinskiy A, Yoon DY, Graf R, Pisula W, Spiess HW, Mullen K (2011) J Am Chem Soc 133:2605
132. Niedzialek D, Lemaur V, Dudenko D, Shu S, Hansen MR, Andreasen JW, Pisula W, Müllen K, Cornil J, Beljonne D (2013) Adv Mat 25:1939
133. Emsley L (2013) J Am Chem Soc 135:8089
134. Bayro MJ, Debelouchina GT, Eddy MT, Birkett N, MacPhee CE, Rosay M, Maas WE, Dobson CM, Griffin RG (2011) J Am Chem Soc 133:13967
135. Lelli M, Gajan D, Lesage A, Caporini MA, Vitzthum V, Miéville P, Héroguel F, Rascón F, Roussey A, Thieuleux C, Boualleg M, Veyre L, Bodenhausen G, Coperet C, Emsley L (2011) J Am Chem Soc 133:2104
136. Spiess HW (2008) Angew Chem Int Ed 47:639
137. Münnemann K, Spiess HW (2011) Nature Phys 7:522
138. Lee SY, Widmann M, Rendler T, Doherty MW, Babinec TM, Yang S, Eyer M, Siyushev P, Hausmann BJM, Lonca M, Bodrog Z, Gali A, Manson NB, Fedder H, Wrachtrup J (2013) Nat Nanotech 8:487
139. Gallagher FA, Kettunen MI, Day SE, Hu DE, Ardenkjaer-Larsen JH, in't Zandt R, Jensen PR, Karlsson M, Golman K, Lerche MH, Brindle KM (2008) Nature 453:940